*Coupled Systems Mechanics, Vol. 1, No. 3 (2012) 247-268*
DOI: http://dx.doi.org/10.12989/csm.2012.1.3.247


# Dynamic response analysis of floating offshore wind turbine with different types of heave plates and mooring systems by using a fully nonlinear model

Muhammad Bilal Waris*[1] and Takeshi Ishihara[2]

[1]*Department of Civil and Architectural Engineering, Sultan Qaboos University, P.O.Box 33, Muscat 123, Sultanate of Oman*
[2]*Department of Civil Engineering, School of Engineering, University of Tokyo, 7-3-1, Hongo, Bunkyo-ku, Tokyo 113-8656, Japan*

*(Received July 25, 2012, Revised August 20, 2012, Accepted September 9, 2012)*

**Abstract.** A finite element model is developed for dynamic response prediction of floating offshore wind turbine systems considering coupling of wind turbine, floater and mooring system. The model employs Morison's equation with Srinivasan's model for hydrodynamic force and a non-hydrostatic model for restoring force. It is observed that for estimation of restoring force of a small floater, simple hydrostatic model underestimates the heave response after the resonance peak, while non-hydrostatic model shows good agreement with experiment. The developed model is used to discuss influence of heave plates and modeling of mooring system on floater response. Heave plates are found to influence heave response by shifting the resonance peak to longer period, while response after resonance is unaffected. The applicability of simplified linear modeling of mooring system is investigated using nonlinear model for Catenary and Tension Legged mooring. The linear model is found to provide good agreement with nonlinear model for Tension Leg mooring while it overestimates the surge response for Catenary mooring system. Floater response characteristics under different wave directions for the two types of mooring system are similar in all six modes but heave, pitch and roll amplitudes is negligible in tension leg due to high restraint. The reduced amplitude shall lead to reduction in wind turbine loads.

**Keywords:** floating offshore wind turbine; coupled system; Morison equation; finite element

## 1. Introduction

Wind energy is one of the most renowned source of renewable energy, with steep hikes in fuel prices, wind energy poses to be an attractive and environment friendly source of power generation. In metropolis areas, where power demand is high, onshore wind resource is sparse and limited land is available for large wind farms. Most of world's metropolises are near shore and offshore wind energy offers the obvious advantage of no land usage and probably more reliable wind resource. To harvest this wind resource, bottom-mounted offshore wind farms have been developed with a capacity of nearly 2500 MW, near 2200 MW are under construction and a further 34,000 MW are

* Corresponding author, Assistant Professor, E-mail: waris@squ.edu.om

proposed (Wikipedia). In Japan, the wind resource in potential bottom-mounted sites is limited (Ishihara and Yamaguchi 2005) and it is essential to employ floating offshore technology, which needs to be borrowed from existing oil and gas (O&G) industry. The O&G systems design is always safety driven and is thus conservative. The structures are very large and heavy with rigid components, due to small response hydrodynamic and aerodynamic damping has small contribution and the mooring system is in linear range. On the other hand, floating wind turbines systems design has to be economy driven and should be optimized. Their floater is much lighter, elements are slender that may lead to elastic deformations and large response, hydrodynamic and aerodynamic damping therefore have significant influence on dynamic response and mooring system needs to be considered in its nonlinear range.

Floating offshore wind turbine systems can be divided into two groups, single turbine system and multi-turbine system. Several initial concepts (Barltrop *et al*. 1993, Handerson and Patel 1998, Bulder *et al*. 2002, Ishihara *et al*. 2007, Phuc *et al*. 2007) considered multi-turbine floaters to reduce floater motion due to smaller thrust height to floater span ratio and improve economy by employing single mooring system to support several wind turbines. However, such systems have to resist high current and wave loads and turbines suffer wake effects. In some research (Tong *et al*. 1993, Bertacchi *et al*. 1994, Jonkman 2007), emphasis is thus laid on floater with single wind turbine considering it more suitable for offshore application. A couple of single wind turbine prototypes have been installed and decommissioned to investigate dynamic response of such systems (Offshore Industry Vol.2, 2009). Due to small size such floaters are subjected to large wave induced response, which leads to nonlinear behaviour of restoring force and mooring system. It is therefore, essential to investigate means such as heave plates and Tension Legged mooring systems to reduce floater response.

The dynamic response characteristics of floating offshore wind turbine systems depend upon its several structural attributes. The most significant are:

· Aerodynamic effects from the rotor.
· Effect of control system of wind turbines.
· Hydrodynamic effects.
· Restoring effects.
· Resonance effect due to elastic deformations.
· Mooring system effect.

To have accurate prediction of dynamic response of floating wind turbine systems, all these attributes should be considered. Henderson and Patel (1998) are one of the first to work on floating wind turbine systems. He investigated the contribution of floater motion to wind turbine tower and blade loads. They applied Morison's equation to large floating systems ignoring hydrodynamic damping and elastic effects. Ishihara *et al*. (2007) and Phuc *et al*. (2007) investigated a multi-turbine floater with slender elements to discuss resonance effects due to elastic deformation. They also investigated contributions of hydrodynamic and aerodynamic damping discussing importance of these factors through comparison with water tank experiment. These studies (Henderson and Patel 1998, Ishihara *et al*. 2007, Phuc *et al*. 2007), however, used linear model for mooring system and employed linear model for restoring force that can have significant effect on small semi-submersible floater having large response. Jonkman (2007) discussed dynamic response for a single turbine barge floater system using an analytical model for Catenary mooring system, but accuracy of the model is not validated through experiment. In view of these studies, it is observed that use of nonlinear models for estimation of all applied forces in a coupled simulation is still required, while

the effect of different types of mooring system models on dynamic responses also needs to be investigated.

In this study, a nonlinear finite element model is developed to investigate dynamic response of floating offshore wind turbine systems considering coupling between wind turbine, floater and mooring system. Section Numerical model discusses the numerical scheme developed and finite element models used in this study. Description of water tank experiment and verifications of the developed finite element model is provided in section Validation of developed model. Finally, the effects of heave plates, applicability of linear and nonlinear models for dynamic response prediction of Catenary and Tension-legged mooring system on floater response are discussed in Section Results and Discussion. The effect of incident wave direction on floater response modes for the two mooring types is also discussed in this section. Effect of response modes of floater on wind turbine loads shall be included in a separate article.

## 2. Numerical model

A finite element scheme that can use beam, truss and spring type elements and can consider full coupled interaction between floater, wind turbine and mooring system is developed in this study. The time domain analysis enables the model to efficiently capture nonlinear effects. Morison equation with Srinivasan's Model is used for estimation of hydrodynamic force on the system, restoring force is investigated using a proposed non-hydrostatic model and mooring force is estimated using nonlinear model considering mooring contact with seabed for Catenary mooring and pre-tension for Tension Leg mooring.

### *2.1 Equation of motion*

The general formulation of equation of motion for the floater system can be written as

$$[M]\{\ddot{X}\} + [C]\{\dot{X}\} + [K]\{X\} = \{F\} \tag{1}$$

Where

$$[M] = \begin{bmatrix} M_T & 0 & 0 \\ 0 & M_F & 0 \\ 0 & 0 & M_M \end{bmatrix}, [C] = \begin{bmatrix} C_{TT} & C_{TF} & 0 \\ C_{FT} & C_{FF} & C_{FM} \\ 0 & C_{MF} & C_{MM} \end{bmatrix}, [K] = \begin{bmatrix} K_{TT} & K_{TF} & 0 \\ K_{FT} & K_{FF} & K_{FM} \\ 0 & K_{MF} & K_{MM} \end{bmatrix}$$

$$\{X\} = \{X_T \;\; X_F \;\; X_M\}^T, \{F\} = \begin{Bmatrix} F_T \\ F_F \\ F_M \end{Bmatrix} = \begin{Bmatrix} F_\gamma \\ F_\gamma \\ F_\gamma \end{Bmatrix} + \begin{Bmatrix} 0 \\ F_\beta \\ F_\beta \end{Bmatrix} + \begin{Bmatrix} 0 \\ F_H \\ F_H \end{Bmatrix} + \begin{Bmatrix} 0 \\ F_R \\ F_R \end{Bmatrix} + \begin{Bmatrix} 0 \\ 0 \\ F_C \end{Bmatrix} + \begin{Bmatrix} F_W \\ F_W \\ 0 \end{Bmatrix} + \begin{Bmatrix} F_B \\ F_B \\ 0 \end{Bmatrix}$$

The subscripts "*T*", "*F*" and "*M*" refer to turbine, floater and mooring system respectively. $\{X\}$, $\{\dot{X}\}$ and $\{\ddot{X}\}$ are unknown displacements in six degree of freedom and their time derivatives. $[M]$ is mass matrix, $[C]$ is damping matrix and $[K]$ is stiffness matrix of the system. $\{F\}$ is total external force vector changing with time. $\{F_\gamma\}$ is gravitational force, $\{F_\beta\}$ is buoyancy force, $\{F_H\}$ is hydro-

dynamic force, $\{F_R\}$ is restoring force, $\{F_C\}$ is seabed contact force, $\{F_W\}$ is aerodynamic force acting on wind turbine and floater system and $\{F_B\}$ is blade element momentum force on the wind turbine rotor during operation. In addition to these forces, mooring force $\{F_G\}$ also needs to be estimated for linear modeling of mooring system.

### 2.1.1 Hydrodynamic force

Morison's equation (Morison *et al*. 1950) is well known for estimation of wave exciting force on slender bottom mounted cylinders. The equation assumes disturbing force due to wave to be composed of inertia and drag force linearly added together and is usually applicable when structure is small compared to wavelength ($D < 0.20\lambda$). For a floating structure, free to oscillate in waves and current, Morison equation is modified by Sarpkaya and Isaacson (1981) as follows

$$\{F_H\} = \{F_{HM}\} + \{F_{HW}\} + \{F_{HD}\} \tag{2}$$

$$\{F_{HM}\} = -[M_a]\{\ddot{X}\} \quad where\ M_a = \rho_w(C_M - 1)V \tag{3}$$

$$\{F_{HW}\} = \rho_w C_M V\{\dot{u}\} \tag{4}$$

$$\{F_{HD}\} = 0.50\rho_w C_D A\{u - \dot{X}\}|\{u - \dot{X}\}| \tag{5}$$

In Eq. (2) first term $F_{HM}$ is added inertia force, second $F_{HW}$ is Froude-Krylov Force and $F_{HD}$ is drag force. In Eqs. (3)-(5) $\rho_w$ is density of water, $M_a$ is added mass. $A$ and $V$ are characteristic area and volume for buoyancy. $\dot{X}$ is velocity of moving element, $u$ and $\dot{u}$ are wave velocity and acceleration. $C_D$ and $C_M$ are hydrodynamic drag and inertia coefficients respectively that depend on cross-sectional shape of the element/member. Henderson and Patel (1998) and Offshore Standard DNV-OS-J101 (2004) showed that these values are functions of Keulegan-Carpenter number $K_c = u_{\max}T/D \approx \pi H/D$ and relative roughness, where $u_{\max}$ is maximum wave particle velocity at still water level and $T$ is wave period. Since relative wave particle velocity as well as first term of wave exciting force contains velocity of moving element, hydrodynamic damping is automatically taken into account. As the Morison's equation cannot predict the vertical force on base of submerged cylinder, Haslum (1999) has proposed that volume of half sphere of water under a vertical cylinder should be considered for added mass as shown in Eq. (6), where $D$ is diameter of the cylinder base.

$$V = 2\pi/3(D/2)^3 \tag{6}$$

In this study, a linear damping ratio of 15% is used following Srinivasan *et al*. (2005). This damping force can be modeled by a pseudo structural damping of the system as represented in Eq. (7).

$$\{F_{HD}\} = -[C_{ED}]\{\dot{X}\} \tag{7}$$

Where $\{\dot{X}\}$ is the vector containing velocity of moving element and $[C_{ED}]$ is a damping matrix. This hydrodynamic damping matrix is estimated using Raleigh's damping model as follows.

$$[C_{ED}] = \alpha([M] + [M_a]) + \beta[K_R] \tag{8}$$

$$\alpha = 2\omega_1\omega_2\left(\frac{\omega_1\zeta_2 - \omega_2\zeta_1}{\omega_1^2 - \omega_2^2}\right), \quad \beta = \left(\frac{\omega_1\zeta_1 - \omega_2\zeta_2}{\omega_1^2 - \omega_2^2}\right) \tag{9}$$

Where $\omega_1$, $\omega_2$ and $\zeta_1$, $\zeta_2$ are natural frequency and damping for heave and pitch modes. $[K_R]$ is the restoring stiffness matrix discussed in next subsection.

### 2.1.2 Restoring force

To estimate restoring force due to vertical displacement of the floater, a non-hydrostatic model [NHM] is proposed and its efficiency *w.r.t* simple hydrostatic model [HM] is verified through comparison with experiment. The restoring force $\{F_R\}$ in Eq. (1) can be estimated using these two models as follows

$$\{F_R\}\big|_{HM} = [K_R]\{X\} \tag{10}$$

$$\{F_R\}\big|_{NHM} = [K_R](\{X\} - \{\eta\}) \tag{11}$$

$$[K_R] = \begin{bmatrix} 0 & 0 & 0 & 0 & 0 & 0 \\ 0 & 0 & 0 & 0 & 0 & 0 \\ 0 & 0 & -\rho_w g A_w & 0 & 0 & 0 \\ 0 & 0 & 0 & -W \times GM_X & 0 & 0 \\ 0 & 0 & 0 & 0 & -W \times GM_Y & 0 \\ 0 & 0 & 0 & 0 & 0 & 0 \end{bmatrix} \tag{12}$$

Where $[K_R]$ is first order hydrostatic restoring force coefficient (Motora *et al*. 1997), $\{X\}$ is displacement vector and $\{\eta\}$ is wave elevation vector, which only has nonzero element for vertical degree of freedom. $g$ is acceleration due to gravity, $A_w$ is cross-sectional area, $W$ is weight of the model, $GM_X$ and $GM_Y$ are meta-centric height of the model in X and Y-directions respectively.

### 2.1.3 Mooring force

The linear model used in this study does not consider coupling between floater and mooring system. If this coupling is not considered, the mooring force $\{F_G\}$ on the floater needs to be investigated. In linear model, mooring system is modeled as linear springs having constant stiffness $[K_G]$ and mooring force is estimated from fairlead displacement $\{X_F\}$ as given in Eq. (13). This method is commonly used due to its ease of modeling in experiment as well as simulation. In this study, springs used to represent this linear stiffness are considered part of the total system and included in total system stiffness.

$$\{F_G\} = -[K_G]\{X_F\} \tag{13}$$

The nonlinear model for Catenary mooring system needs to consider the interaction of mooring line and seabed. The contact force $\{F_C\}$ acts on portion of the mooring system in contact with seabed. This force is divided into normal $F_n$ and tangential $F_t$ components with respect to mooring line and estimated as follows

$$\{F_C\} = \begin{Bmatrix} F_t \\ F_n \end{Bmatrix} = \begin{bmatrix} 0 & \mu k \\ 0 & k \end{bmatrix} \begin{Bmatrix} U \\ V \end{Bmatrix} \tag{14}$$

Where $\mu$ is coefficient of friction, $U$ and $V$ are relative displacements in tangential and normal direction respectively and $k$ is penalty constant. According to Ju *et al*. (1995), Eq. (14) can be modified to Eq. (15) for the condition that $U \approx 0$.

$$\{F_C\} = \begin{Bmatrix} F_t \\ F_n \end{Bmatrix} = k \begin{bmatrix} \mu^2 & \mu \\ \mu & 1 \end{bmatrix} \begin{Bmatrix} U \\ V \end{Bmatrix} \tag{15}$$

The contact force at each node lying on seabed is estimated through Eq. (15) and Newton-Raphson iterations are used for convergence. The nonlinear model for Tension Leg mooring needs to model effect of element pre-tension, considered using the model explained in Cook *et al*. (1989).

#### 2.1.4 Aerodynamic force

The developed model considers aerodynamic loads acting on wind turbine using quasi-steady theory, in which aerodynamic drag, lift and moment are estimated using aerodynamic drag, lift and moment coefficients. The rotation of the wind turbine has been modeled using blade element and momentum theory, considering blade tip loss, hub loss and tower shadow. Details of these models are described in the Waris (2010), and not included in here since wind is not considered in this discussion.

### 2.2 Numerical scheme

For numerical solution rewriting Eq. (1) as

$$([M] + [M_a])\{\ddot{X}\} + ([C] + [C_{ED}])\{\dot{X}\} + [K]\{X\} = \{F_\gamma\} + \{F_\beta\} + \{F_H\} + \{F_R\} + \{F_C\} + \{F_W\} + \{F_B\} \tag{16}$$

A model based on Eq. (16) is developed to predict dynamic response of floating offshore wind turbine system. $\{F_R\}$ can be estimated using hydrostatic model or non-hydrostatic model. $\{F_G\}$ for linear model is considered using spring elements and included on the left hand side of equation. The structural damping matrix is estimated using the Caughey Series (Caughey 1960, Wilson and Penzien 1972) as shown in Eq. (17).

$$[C] = [M] \sum_{k=0}^{p} a_k ([M]^{-1}[K])^k, \quad \zeta_i = \frac{1}{2}\left[\frac{a_0}{\omega_i} + a_1 \omega_i + a_2 \omega_i^3 + \cdots + a_{p-1} \omega_i^{2p-3}\right] \tag{17}$$

Where $\omega_i$ and $\zeta_i$ are natural frequency and damping for the $i^{th}$ mode. In this study, a structural damping of 0.50% corresponded to floater and the series is only considered up to 2nd order ($p = 2$). A summary of the numerical model is presented in Table 1.

### 2.3 Finite element model

Finite element model for the floater system is shown in Fig. 1. The floater and wind turbine are

Table 1 Description of the finite element numerical scheme

| | |
|---|---|
| Dynamic analysis | Direct Numerical Integration (Newmark-$\beta$) |
| Formulation | Total Lagrangian formulation |
| Convergence | Newton-Raphson Method |
| Damping estimation | Caughey Series (2nd Order) |
| Element type | Beam (12-DOF) , Truss (8-DOF), Spring(6-DOF) |
| Hydrodynamic force | Morison Equation + Srinivasan Model |
| Restoring force | Hydrostatic / Non-Hydrostatic Model |
| Mooring force | Linear / Nonlinear Model |

Table 2 Description of FE-model used in the study

| Component | Description | | No. of Element | Type |
|---|---|---|---|---|
| Wind turbine | Tower | | 13 | Beam |
| Floater | | | 109 | Beam |
| Mooring system | Experimental setup | Elastic band | 4 | Spring |
| | | kevlar | 24 | Truss |
| | catenary mooring | | 30 / line | Truss |
| | Tension leg mooring | | 10 / tether | Pre-stressed Beam |

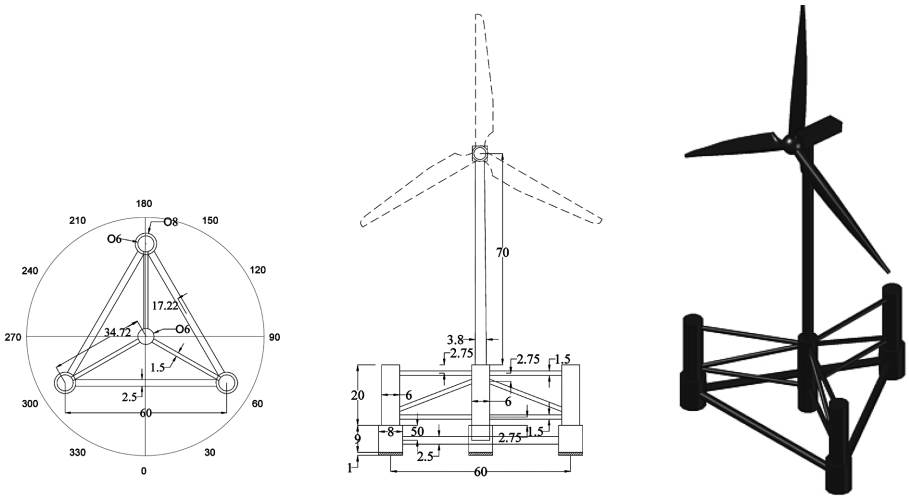


(a) Plan view (b) Front view (c) 3D- view

Fig. 1 Floater model

modeled using beam elements having 122 elements and 114 nodes. Blades are not modeled as wind is not considered and their weight is considered to be concentrated at the nacelle. The mooring arrangement for the experiment (Fig. 4) and two types of mooring systems (Fig. 3) are also modeled. The Distribution of elements in different components of the floating wind turbine system is listed in Table 2. The configuration of the heave plates on the corner columns is represented in Fig. 2. Mass is considered to be concentrated on nodes. $C_D$ and $C_M$ the hydrodynamic drag and inertia coefficients for the floater are considered functions of Kevlegan-Carpenter number '$K_C$' as

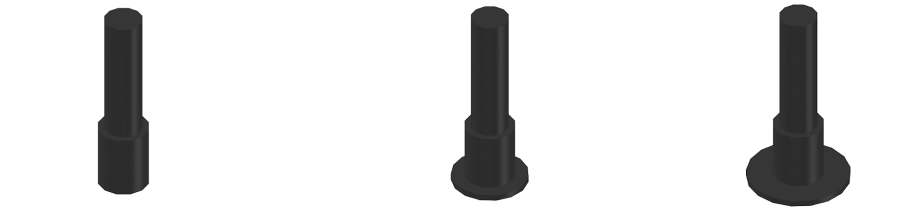

(a) Without Heave Plate [D8] (b) 12cm-Heave plate [D12] (c) 16cm-Heave plate [D16]

Fig. 2 Location of heave plate on corner column

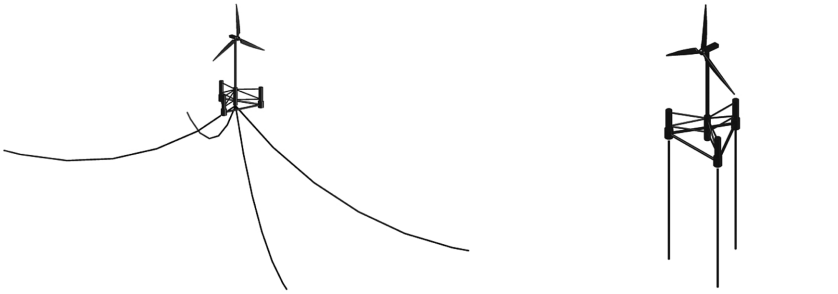

(a) Catenary mooring system (b) Tension leg mooring system

Fig. 3 Types and arrangement of Mooring systems [Section 4.2]

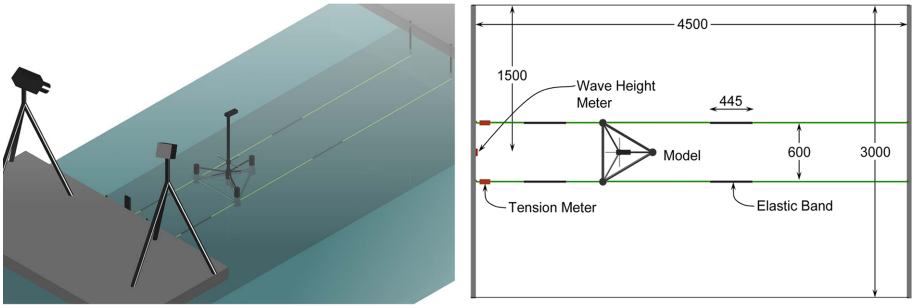


(a) Model setup (b) Experiment configuration (dimension: mm)

Fig. 4 Water tank experiment setup

recommended by Offshore Standard DNV-OS-J101 (2004). Therefore, FE-models are prepared considering two wave heights of 4 cm and 12 cm and the three models i.e., model without heave plates and two models with 12 cm and 16 cm heave plates. The values of $C_D$ and $C_M$ used in simulation are given in Table 3. For the mooring lines $C_D$ and $C_M$ value of 2.6 and 2.0 respectively are used (Chakrabarti 2005).

### 2.4 Wave modeling

For regular waves, the wave particle velocity and accelerations are generated through linear Airy wave theory (Chaplin), simulations were also carried out for nonlinear Stream function theory (Chaplin), but results using the two theories are identical therefore ones from linear theory will be

Table 3 $C_D$ and $C_M$ values used in simulation

| Wave height | D (m) | Bracing | | Central column | Corner Column | | Base plate on corner column | | |
|---|---|---|---|---|---|---|---|---|---|
| | | Inner bracing | Outer bracing | | Top | Base | Without plate | 12 m Plate | 16 m Plate |
| | | 1.5 | 2.5 | 6.0 | 6.0 | 8.0 | 8.0 | 12.0 | 16.0 |
| 4 m | $K_c = \pi H/D$ | 8.40 | 5.00 | 2.10 | 2.10 | 1.60 | 1.60 | 1.05 | 0.80 |
| | $C_D$ | 0.72 | 0.65 | 0.65 | 0.65 | 0.00 | 0.00 | 0.00 | 0.00 |
| | $C_M$ | 1.97 | 2.00 | 2.00 | 2.00 | 2.00 | 2.00 | 2.00 | 2.00 |
| 12 m | $K_c = \pi H/D$ | 25.10 | 15.10 | 6.30 | 6.30 | 4.70 | 4.70 | 3.10 | 2.40 |
| | $C_D$ | 0.71 | 0.83 | 0.66 | 0.66 | 0.65 | 0.65 | 0.65 | 0.65 |
| | $C_M$ | 1.72 | 1.87 | 2.00 | 2.00 | 2.00 | 2.00 | 2.00 | 2.00 |

discussed. For Irregular waves, a modified JONSWAP spectrum (Chakrabarti 1987) is used to generate irregular wave velocity and acceleration history. The spectrum is given as

$$S(\omega) = \alpha^* H_S^2 \cdot \frac{T_P}{2\pi}\left(\frac{\omega T_P}{2\pi}\right)^{-5} exp\left[-1.25\left(\frac{\omega T_P}{2\pi}\right)^{-4}\right] \cdot \gamma^{exp\left[-\frac{1}{2\tau^2}\left(\frac{\omega T_P}{2\pi}-1\right)^2\right]} \tag{18}$$

$$\alpha^* = \frac{0.0624}{0.230 + 0.0336\gamma - 0.185/(1.9+\gamma)} \tag{19}$$

Where $\omega$ is the angular frequency of wave, $H_S$ is significant wave height, $T_P$ is peak wave period, $\gamma$ is peak factor and $\tau$ is the shape factor ($\tau = \tau_a$ for $\omega \le 2\pi/T_P$ and $\tau = \tau_b$ for $\omega > 2\pi/T_P$). The values used in this study are $\tau_a = 0.07$, $\tau_b = 0.09$ according to Chakrabarti (1987). The peak period is dependent on the significant wave height, one of the ways to estimate its value for a given value of $\gamma$ is presented in Chakrabarti (1987) as

$$T_P = \sqrt{\frac{H_S}{(0.11661 + 0.01581\gamma - 0.00065\gamma^2)}} \tag{20}$$

As the structural response is a function of both wave height and wave period, it is important to keep one of these parameters constant to study the effect of the other. Therefore in order to keep the significant wave height nearly constant, different values of $\gamma$ are considered to obtain different peak wave periods in section 4.2. This approach deviates for general practice of using a constant $\gamma$, however the intension there is comparison of two models over a range of wave period with little variation in wave height.

## 3. Validation of developed model

Validation of the nonlinear numerical model developed in this study using a single experiment is very difficult. Therefore, the developed model has been verified in parts using experiments designed to investigate a particular component of the numerical model. A water tank experiment discussed in 3.1 is performed to verify performance of the non-hydrostatic model. The contact model and pre-

tension model are verified using experimental data for respective cases.

### 3.1 Water tank experiment

The water tank experiment is performed on a semi-submersible type floater with single wind turbine under regular wave conditions using two heave plate sizes. Considering Froude's Number similarity 1:100 scale is selected for the experiment. The discussion in this paper is, however, done using normalized values of displacement and forces. The floater (Fig. 1) is statically stable at submerged depth of 20 cm. Wave heights of 4 cm and 12 cm corresponding to rated and extreme sea condition respectively are considered in the experiment. This experiment does not consider wind, as influence of aerodynamic damping has already been discussed in previous study (Ishihara *et al*. 2007, Phuc *et al*. 2007). The wind turbine blades are therefore not required and weight of blades is included in the nacelle. Two heave plate sizes, with 1.5 and 2.0 times diameter of original floater's base is considered. The physical properties of the three models are listed in Table 4. The values enclosed in brackets represent values measured during experiment.

The experiment is carried out in 15 m long and 3 m wide tank with water depth of 1.5 m (NMRI Facility). Fig. 4 shows the model layout in water tank. The experiment is setup between two fixed panels over the water tank that support CCD camera used for measurement of displacement, wave height meter and the mooring setup. The model is placed at the center of the tank and is connected to elastic bands through Kevlar thread which is connected to tension meter at front. At the rare, a pulley and weight are used to develop required initial tension of 2.95 N that produces a linear

Table 4 Properties of the Experiment Model

| Heave plate | Corner column base diameter (cm) | Weight (kg) | Moment of inertia (Kg-m$^2$) | Center of gravity* (cm) | Center of buoyancy* (cm) | Meta-centric height (cm) |
|---|---|---|---|---|---|---|
| Nil | 8.0 | 3.80 | 0.198 | 5.13 | 11.30 | 8.40 (8.80) |
| 12 m | 12.0 | 4.06 | 0.211 | 5.93 | 11.70 | 8.10 (8.30) |
| 16 m | 16.0 | 4.375 | 0.230 | 6.90 | 12.20 | 7.70 (8.00) |

*With reference to still water level
() Measured data

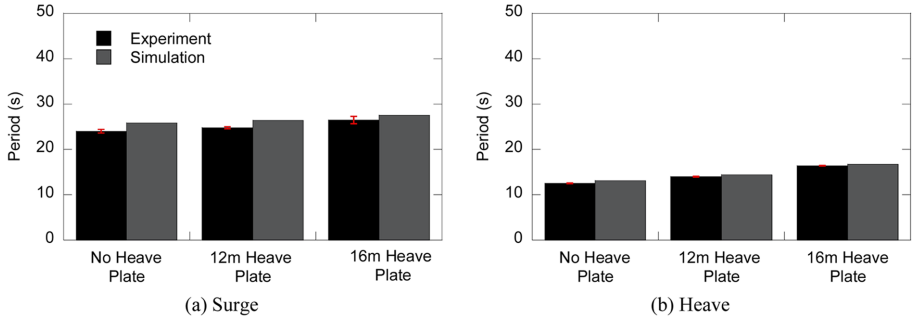


Fig. 5 Comparison of observed and predicted natural periods

stiffness of 45 N/m in surge direction. The linear mooring stiffness used in the experiment is estimated for the Catenary mooring arrangement shown in Fig. 3(a) using steady wave and current analysis (Ishihara *et al*. 2007). As the experiment is unidirectional and mooring stiffness in heave direction is negligible, only stiffness in surge direction is considered. Displacements are measured

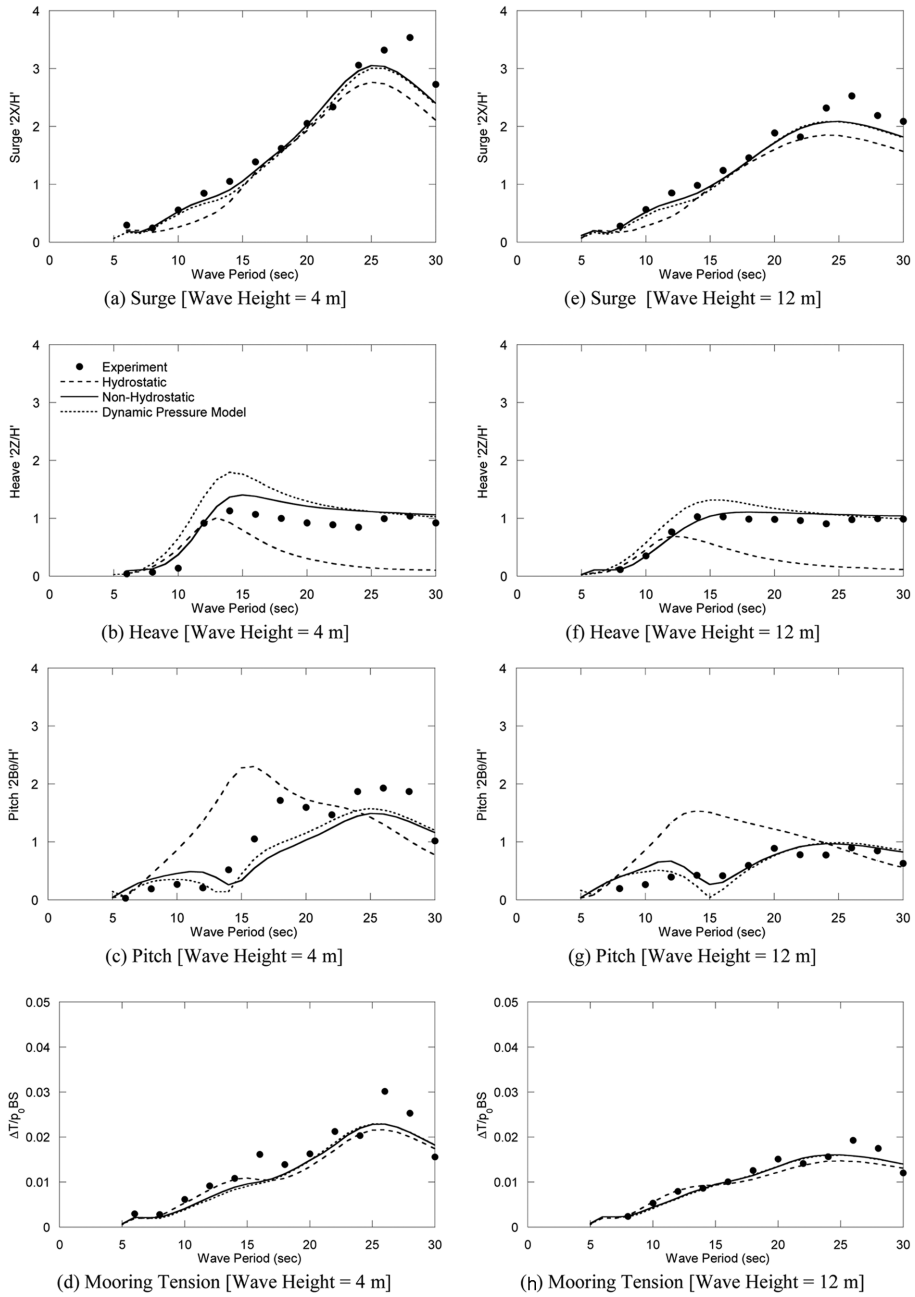


(a) Surge [Wave Height = 4 m] (e) Surge [Wave Height = 12 m]

(b) Heave [Wave Height = 4 m] (f) Heave [Wave Height = 12 m]

(c) Pitch [Wave Height = 4 m] (g) Pitch [Wave Height = 12 m]

(d) Mooring Tension [Wave Height = 4 m] (h) Mooring Tension [Wave Height = 12 m]

Fig. 6 Comparison of predicted and measured responses for model without heave plates

from a four-legged LED target fixed to the wind turbine tower. The data collection is done at 30 Hz for 60 sec. Regular waves with period range 0.6~3.0 sec are considered at intervals of 0.20 sec.

### 3.2 Non-hydrostatic model for restoring force

Prior to verification of the non-hydrostatic model, it is essential to calibrate/ verify the FE-model used in the simulation. Free vibration tests are carried out during experiment to estimate natural periods of floating wind turbine system in surge and heave modes. Similarly, free vibration test are simulated using the FE-model. Estimation of $C_D$ and $C_M$ values for FE-models in free vibration test is based on element velocity '$U$' and period '$T$' estimated from free vibration experiment. Fig. 5 shows comparison of observed and predicted natural period in surge and heave modes for prototype scale. The error bars represent variation in experimental results over a set of 20 observations. The maximum difference in predicted and observed is about 5%. The FE-models are therefore, in acceptable agreement with the actual experiment models.

To verify performance of non-hydrostatic restoring force model, it is compared with the hydrostatic model and dynamic vertical pressure model under vertical columns. The comparison is done considering the original floater (without heave plates). Fig. 6 shows comparison of surge, heave and pitch response amplitudes for the three models with experiment data for 4.0 m and 12.0 m wave heights. The corresponding mooring tension amplitudes are also presented. The tension amplitude is normalized by product of hydrodynamic pressure $p_0$ at the water surface and the projected area of the floater. The projected area estimated as the product of floater span '$B$' and submerged depth '$S$'. The dynamic wave pressure '$p_0$' at water surface is estimated using linear wave theory as $p_0 = \rho g H / 2$. The three models provide similar results for surge, while hydrostatic model underestimates and dynamic vertical pressure model overestimates heave response after resonance peak. The non-hydrostatic model gives better agreement with experiment compared to the other models for heave. In addition to surge and heave response, pitch response of the floater is also very critical mode of motion for floating wind turbine systems. The response is normalized with respect floater span "B" and wave height "$H$". It can be observed that dynamic pressure model and non-hydrostatic model provide similar results while hydrostatic model overestimates pitch near response state. The three models provide similar agreement with experiment for mooring tension since line tension is independent of vertical response in the experimental arrangement considered.

To understand the better results of non-hydrostatic model, total vertical force on the floater system is investigated comparing it with hydrostatic model. Considering Eq. (1), as gravitational and

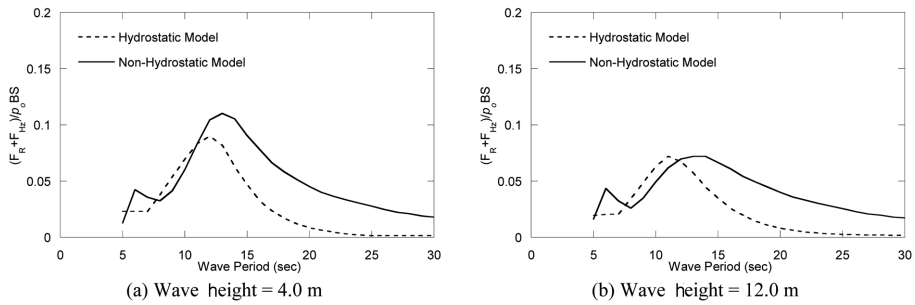


(a) Wave height = 4.0 m (b) Wave height = 12.0 m

Fig. 7 Comparison of total vertical force obtained by hydrostatic and Non-Hydrostatic Model for model without heave plates

buoyancy force cancel out and no wind and contact force acts on the floater in this case, the total vertical force is sum of restoring force and hydrodynamic force in vertical direction '$F_R + F_{HZ}$'. This force is responsible for heave response as no mooring force is considered in vertical direction. The dynamic line tension '$\Delta T$' is normalized with respect to the incident hydrodynamic force $p_0BS$ discussed earlier. Comparison of this force for the two models is shown in Fig. 7. It can be observed, that before resonance peak, hydrostatic model provides good prediction of total vertical force while afterwards it underestimates this force resulting in underestimation of response amplitude. The non-hydrostatic model is therefore clearly the better choice for response prediction of a such small sized floaters.

### 3.3 Nonlinear model for mooring system

The performance of the contact model is verified through an experiment using a Catenary chain. A chain 11.6 g/m in weight and 2.0 m in length is suspended between two supports with horizontal span of 1.5 m. The chain thus freely hangs under its own weight, with mid-span sag of $\approx 0.60$ m as shown in Fig. 8(a). A plate is raised from underneath this Catenary to achieve different contact lengths between the plate and chain. Four plate elevations of 0.55, 0.50, 0.45 and 0.403 m are considered, where elevation is measured downwards from Catenary support. Developed model is used to reproduce this Catenary arrangement using 80 truss elements. Fig. 8(b) shows comparison of profile from experiment and simulation for free Catenary and for plate elevation $Z = 0.403$ m, while Fig. 8(c) shows comparison of contact lengths at four plate elevations. The comparison indicates that the developed tool can correctly model the chain profile and contact lengths for the

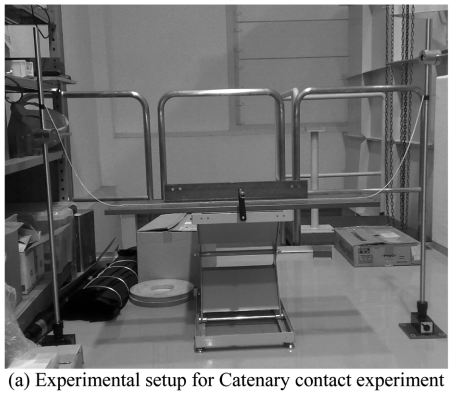

(a) Experimental setup for Catenary contact experiment

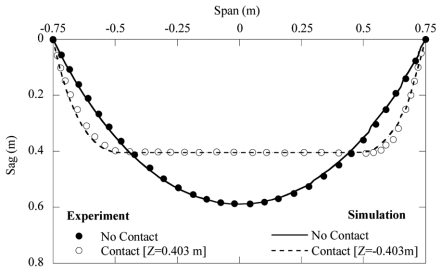


(b) Profile shapes for chain

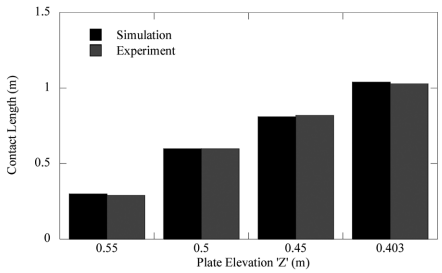


(c) Contact length with horizontal plate

Fig. 8 Verification of contact model for seabed interaction

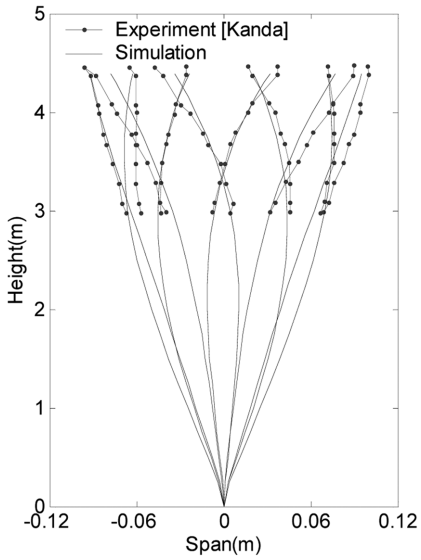


Fig. 9 Verification of initial tension model

Catenary chain. As the forces on the fairlead and at anchor level are function of mooring line profile, it shows that developed tool can be used to accurately predict the mooring forces on the floater and in mooring system.

For nonlinear modeling of tethers in Tension Leg mooring system, tether pretension is very important. The developed tool can consider element pretension and its performance is verified using experimental data from Kanda *et al*. (1998). The reference experiment was performed on a 1:100 scaled submerged tether model having length of 4.391 m and initial pre-tension of 21.60 N. The FEM model of the tether is prepared using 20 pre-tensioned beam elements and is verified with experimental model using Eigen-value analysis. The tether is subjected to a harmonic forced vibration of 100 mm amplitude at 1.28 sec, which is the first mode of vibration. The comparison of tether profiles over a cycle of vibration at interval of 0.133 sec is shown in Fig. 9. It can be observed that developed model shows good agreement with experiment. The developed tool is therefore completely verified and can be used for response prediction of fully coupled floating offshore wind turbine systems.

## 4. Results and discussion

In this section, results from water tank experiment and numerical simulation for response characteristics of the floating offshore wind turbine system are discussed. First, the effect of heave plates on the dynamic response is studied, then effect of models for mooring system considering Catenary and Tension Leg mooring system under regular and irregular waves is investigated and finally sensitivity of floater response to mooring type under different wave direction is evaluated. The discussion therefore emphasis on means to reduce the response of small and light floating offshore wind turbine systems and investigate the applicability of linear and nonlinear models.

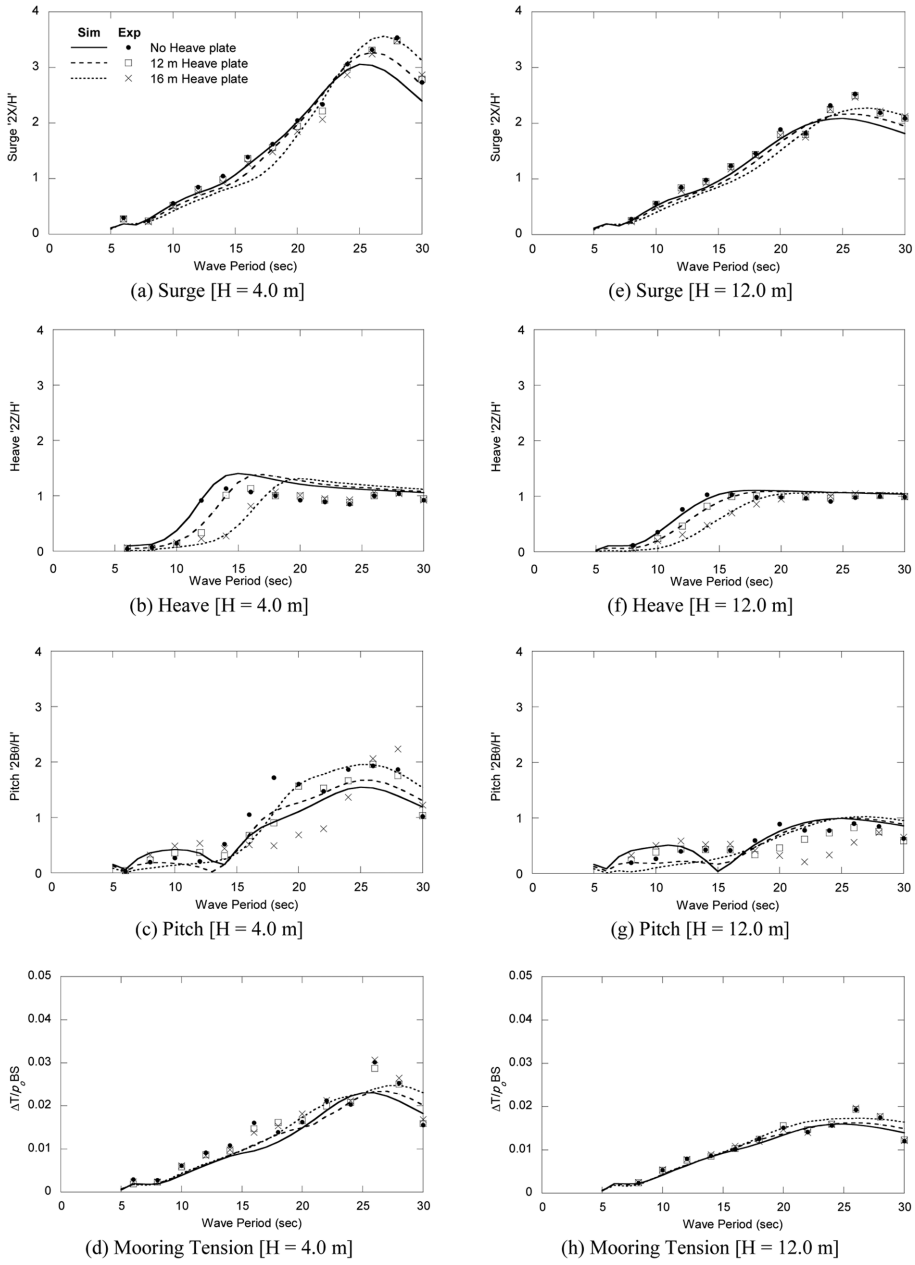


Fig. 10 Influence of heave plate on floater response

### *4.1 Influence of heave plates on floater dynamic response*

The influence of heave plates on floater response is discussed using two plate sizes, 1.5 and 2.0 times the original floater diameter. Fig. 10 shows comparison of surge, heave and pitch response for the three models along with mooring line tension for wave height of 4.0 and 12.0 m respectively. Experiment data is plotted with markers and simulation results using non-hydrostatic model

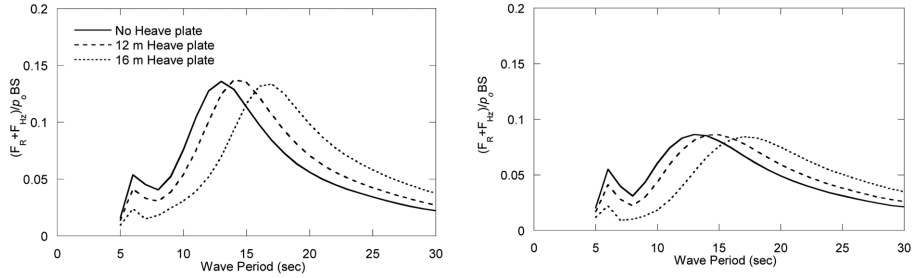


(a) Wave Height = 4.0 m (b) Wave Height = 12.0 m

Fig. 11 Influence of heave plates on total vertical force

are plotted using lines. The surge response is found to be insensitive to presence of heave plates, whoever the effect of hydrodynamic damping is evident with increase in wave height. The heave response demonstrates a shift in resonance peak with inclusion of heave plate. The pitch response for the three models show similar trends with increase in pitch amplitude at resonance with increase in heave plate diameter for 4.0 m wave height. This effect is diminished for 12.0 m wave height owing to increased hydrodynamic damping. The mooring line tension is found to be a function of the surge response and is therefore independent of the presence of heave plates.

The heave plates increase system stiffness in heave mode, which lead to increase in its natural period. In order to understand the influence of heave plates, the total vertical force '$F_R + F_{HZ}$' is considered as shown in Fig. 11. This force is normalized with dynamic wave force $p_0BS$. It can be observed that heave plates reduce this vertical force on the system, which results in reduced response before the resonance peak. After resonance, a larger force is required to develop the same response because of the increased restoring stiffness. It is also important to observe here that after the resonance peak, heave response has nearly same amplitude as the incident wave ($2Z/H \approx 1$). Therefore, heave plates can be used to shift the resonance peak in low energy region of the wave spectrum and cannot reduce the response after natural period of the system. The pitch response prediction for cases with heave plates, therefore in following discussion is only made for the floater model without heave plates.

### 4.2 Influence of mooring systems on floater dynamic response

In previous section, linear model for mooring force is used to discuss the effect of heave plates and non-hydrostatic characteristic of restoring force. Now, influence of mooring system model is discussed using linear and nonlinear model for Catenary and Tension Leg Mooring systems. For Catenary mooring, the experimental setup represents the linear model while Fig. 3(a) represents nonlinear model. In this Mooring system, each mooring line has a length of 660 m and weighs 116 Kg/m with water depth of 150 m. In order to clarify the difference between the two models, response under regular as well as irregular wave conditions is considered. According to recommendations of IEC, simulation period of 1 hour is used in this study for irregular waves. Using Eq. (20), a peak wave period range of 8.0-50.0 sec is considered for significant wave height $H_S = 4.0$ m. In this section as the intent is to understand the effect of modeling mooring system only wave height of 4.0 m is used.

Fig. 12 shows the comparison of two methods of modeling mooring system under regular and irregular waves over a period range up to 50.0 sec. Figs. 12(a) to (c) show the predicted surge,

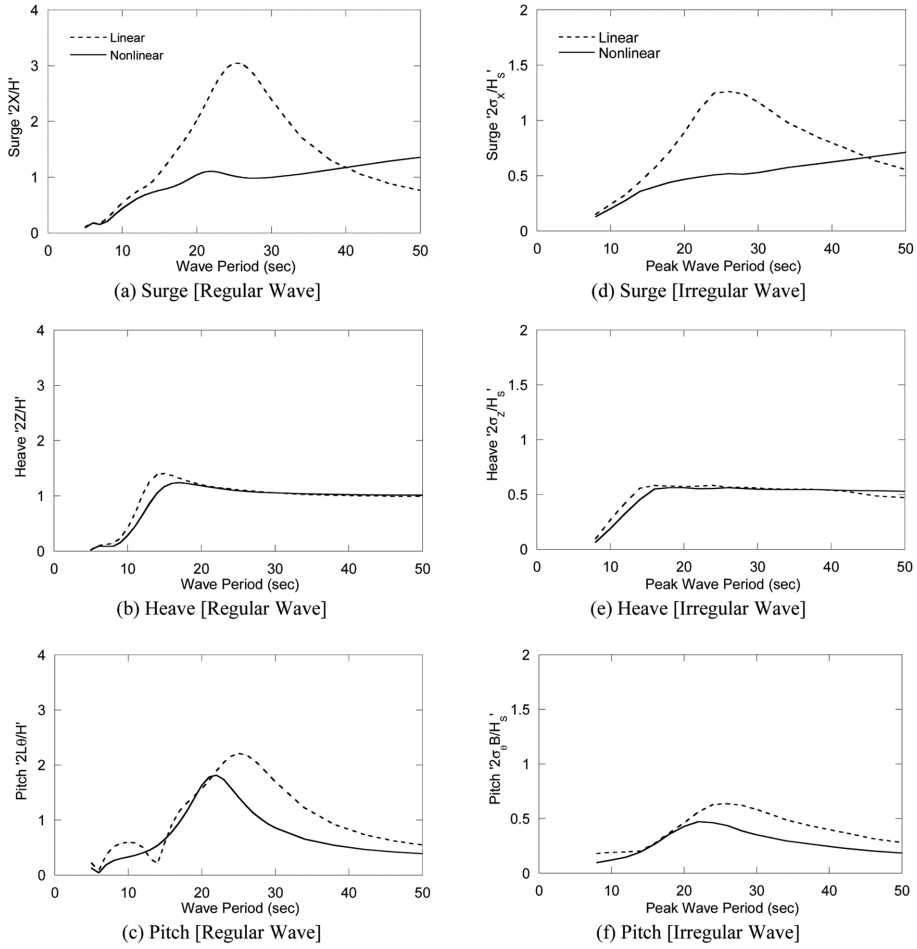


Fig. 12 Linear and nonlinear model for Catenary Mooring System

heave and pitch response amplitude for the floater under regular wave, while Figs. 12(d) to (f) is standard deviation of response in respective modes under irregular waves. The resonance peak observed in surge response using linear model is flattened out in nonlinear model, this is because of nonlinear behaviour of mooring system. The mooring stiffness increases with increase in floater's surge amplitude and change natural period of the system, therefore eliminating resonance effect observed using linear model. The heave response is quite similar for both models as Catenary mooring system does not offer much restraint in vertical direction. The nonlinear model, however, shows slightly reduced heave response amplitude at resonance peak compared to linear model. This reduced response is because of drag and inertia effect on mooring line that affect the heave response. The pitch response is also slightly overestimated by linear model and is observed to resonate with surge response and has overestimation, as can be expected.

Fig. 13(a) shows the comparison of predicted horizontal component of dynamic tension $\Delta T$ normalized with respect to $p_0BS$. For linear model, tension in Kelvar thread is considered as the horizontal component of tension. In nonlinear model, front and rear mooring lines show different amplitudes of dynamic tension that are plotted separately. It can be observed that linear model cannot

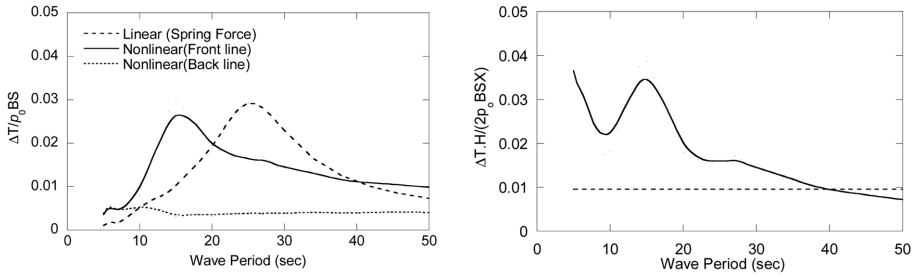


(a) Mooring Line Tension (b) Mooring Stiffness

Fig. 13 Comparison of mooring stiffness in linear and nonlinear model for Catenary Mooring

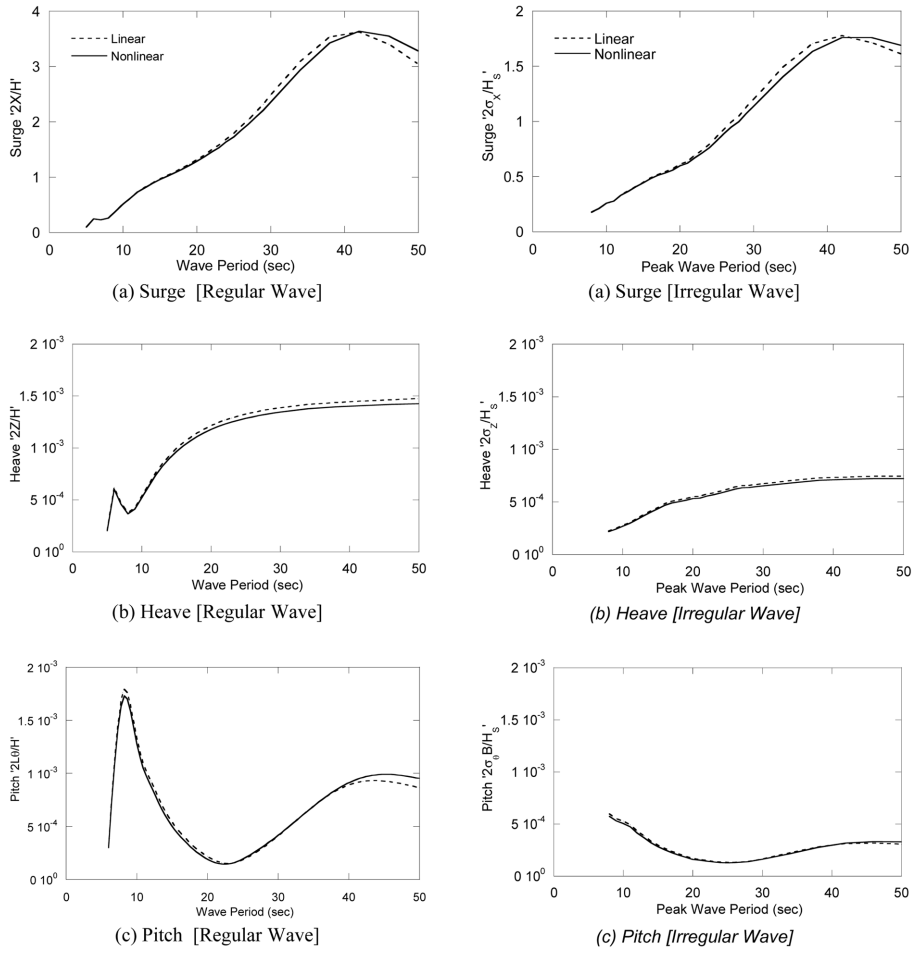


(a) Surge [Regular Wave] (a) Surge [Irregular Wave]

(b) Heave [Regular Wave] *(b) Heave [Irregular Wave]*

(c) Pitch [Regular Wave] *(c) Pitch [Irregular Wave]*

Fig. 14 Linear and Nonlinear Model for Tension Leg Mooring System

reproduce the characteristics of dynamic tension. Using Figs. 12(a) and 13(a) the normalized mooring stiffness for two models can be estimated as given in Fig. 13(b). The Comparison of the mooring stiffness shows that dynamic tension has a significant contribution to mooring stiffness.

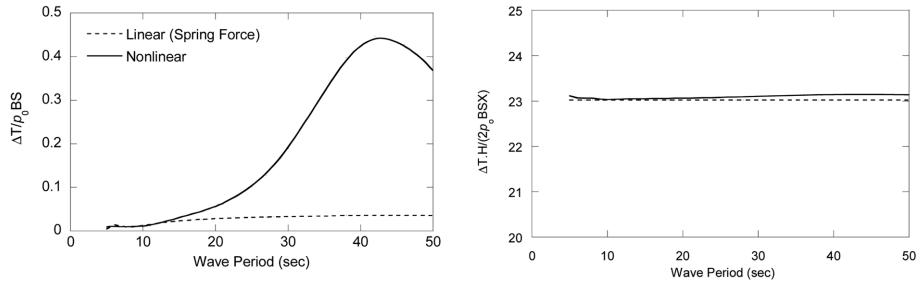


(a) Mooring Line Tension (b) Mooring Stiffness

Fig. 15 Comparison of Mooring stiffness in linear and nonlinear model for Tension Leg Mooring

In order to understand modeling methods for Tension Leg mooring, linear model is compared with the previously verified nonlinear model for Tension Leg configuration shown in Fig. 3(b). The linear model used here considers initial tension and axial stiffness for estimation of linear mooring stiffness using $T_0 / L + EA / L$, where '$L$' represents the length of the tether. The dynamic component of tension is estimated using this linear stiffness and floater displacement. The mooring arrangement and sectional properties of tether are based on Shimada *et al*. 2010. The mooring arrangement consists of two tethers connected to each corner floater, each having an initial tension $T_0 = 2290\ KN$ and $A = 9270\ \text{mm}^2$ with water depth of 150 m. A comparison of surge, heave and pitch response of the two models for 4.0 m wave height under regular and irregular waves is shown in Fig. 14 and normalized dynamic tension and mooring stiffness are presented in Fig. 15. Here it is observed that the linear model provides very good agreement for response but it underestimates the dynamic tension (Fig. 15(a)) in the tether at larger wave periods. Since the contribution of the dynamic tension to mooring stiffness (Fig. 15(b)) is negligible the linear model is able to provide good prediction of response for Tension Leg mooring.

### *4.3 Influence of wave direction on floater dynamic response*

So far in this discussion, emphasis is laid on the three response modes (surge, heave and pitch) that have dominant contribution under unidirectional waves. Estimation of contribution of other modes and dependency of all floater response modes on mooring system under different wave direction is essential and is done here. The extreme sea state with wave height of 12.0 m and wave period of 14.0 sec is considered. The six degrees of freedom of the floater are considered with respect to global coordinate system as *X*-, *Y*-, *Z*- translations and rotations. For a wave inclination of $0^o$ *X*-, *Y*-, *Z*- translations ($\delta_X$, $\delta_Y$, $\delta_Z$) represent Surge, Sway and Heave respectively, while *X*-, *Y*-, *Z*- rotations ($\theta_X$, $\theta_Y$, $\theta_Z$) represent Roll, Pitch and Yaw. The criterion for division of the wave horizon is different in Japan and Europe. In Japan, 16 sectors are used and in Europe 12 sectors are considered. This research considers 12 sectors as shown in Fig. 1(a), so that results are in compliance with European practice and because symmetry for the selected floater system occurs at intervals of 60 degrees around the horizon. Fig. 16 shows translational and rotational amplitude of the floater for Catenary (Cat) and Tension leg (TLP) type mooring system. The translational response amplitudes are normalized with wave amplitude '$H$' and rotational amplitudes with floater span '$B$' and wave amplitude. To understand the dynamic response characteristics of Catenary and Tension Legged Mooring system in all modes, negligible amplitudes from Tension legged mooring system are

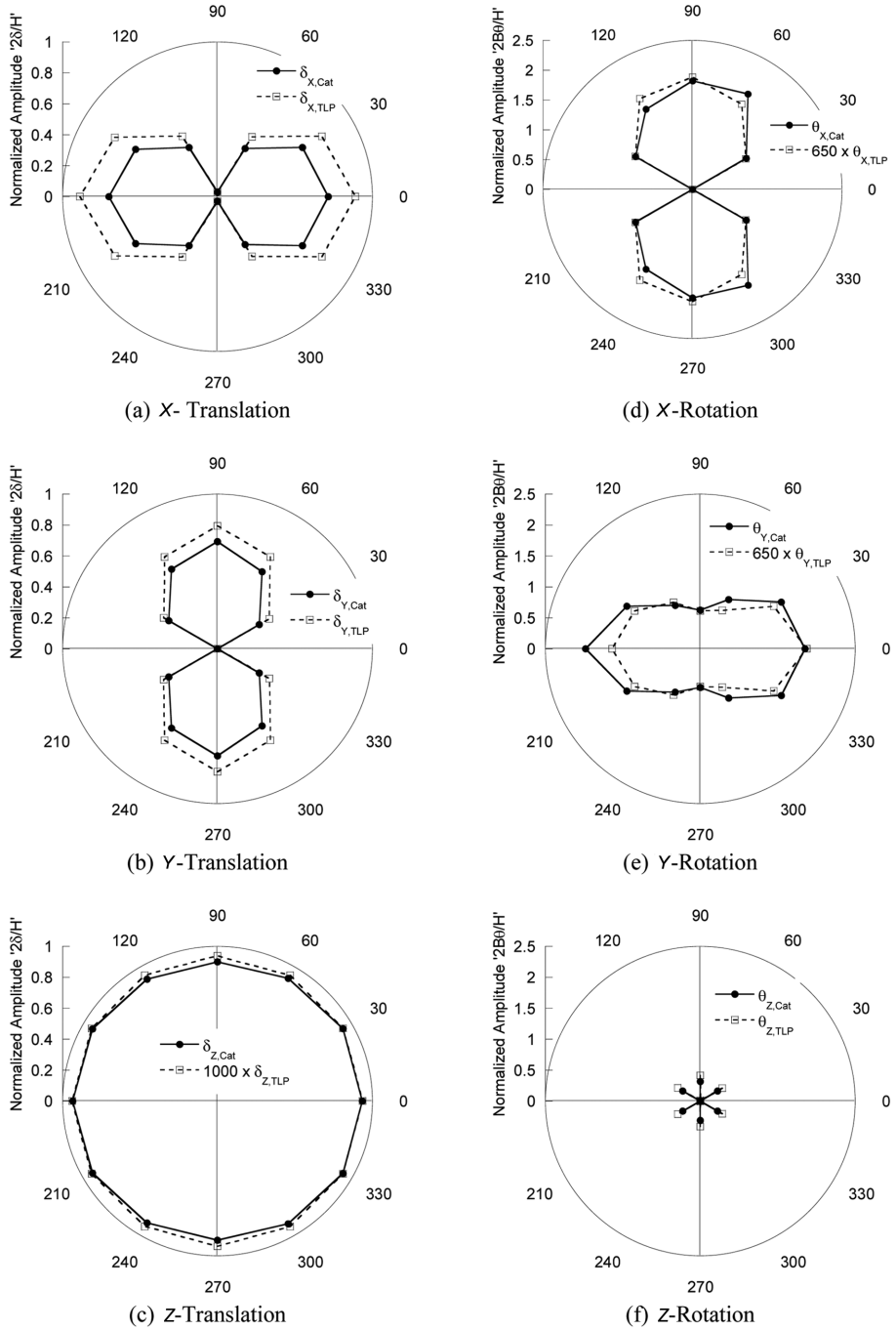


(a) *X*- Translation (d) *X*-Rotation

(b) *Y*-Translation (e) *Y*-Rotation

(c) *Z*-Translation (f) *Z*-Rotation

Fig. 16 Influence of Wave direction on floater response

multiplied with suitable constants to be able to compare them with Catenary system in respective mode. The constants used are 1000 for *Z*-translation and 650 for *X*- and *Y*- rotation. It can be observed that the two types of mooring system essentially have the same characteristics behaviour

with change in wave direction. The magnitude of response is however, dependent on the amount of restraint available. The surge and sway are interdependent and resultant along wave translational amplitude is almost constant. A similar trend can be observed for pitch and roll amplitude. The yaw mode is only excited if the floater is asymmetric about the wave direction and seems to be independent of mooring system. These results show that the vertical and along wave translational response (resultant of surge and sway) is independent of wave direction and however there amplitude is dependent on restraint provided by mooring system. The characteristics of heave and yaw response of floater are independent of mooring system but still amplitude is dependent on restraint. The effect of wave direction on floater response characteristics can be minimized by using a symmetric floater and mooring arrangement, but amplitudes can only be reduced by increasing restraint. Since, Tension Legged mooring system reduce pitch, roll and heave of floater, associated loads on wind turbine can be reduced, leading to economical design for wind turbine.

## 5. Conclusions

A nonlinear FEM model is developed that considers coupled dynamic response of floating wind turbine systems with non-hydrostatic model for restoring force and nonlinear model for mooring systems. The conclusions are summarized as follows:

· The models developed in the study are verified through comparison with water tank tests and show good agreement with experiments. The hydrostatic model underestimates heave response after resonance peaks due to underestimation of restoring force.

· The heave plates have significant effect on heave response and natural period of floating system in heave mode is increased with increase in heave plate size. After the resonance peak, the heave response becomes synchronous with wave amplitude in any case and increased restoring stiffness due to heave plates becomes ineffective.

· The comparison of dynamic responses by linear model and nonlinear model for Catenary and Tension leg mooring system in regular and irregular waves shows that simplification of mooring stiffness to linear spring overestimates surge response at resonance state for the Catenary mooring system and provides good agreement for Tension Leg mooring system, because the initial tension is much larger than the dynamic tension in the Tension Leg mooring system.

· Floater response characteristics for the two types of mooring system are found to be similar because of floater and mooring system symmetry. The amplitudes for surge, sway and yaw modes are also quite similar, while Tension leg system has very high restraint against heave, pitch and roll response.

## References

Barltrop, N. (1993), "Multiple floating offshore wind farm (MUFOW)", *Wind Eng*., **17**(4), 183-188.

Bertacchi, P., Di Monaco, A., de Gerloni, M. and Ferranti, G. (1994), "ELOMAR-A moored platform for wind turbines", *Wind Eng*., **18**(4), 189-198.

Bulder, B.H., van Hees, M.T., Hendeson, A., Huijsmans, R.H.M., Pierik, J.T.G., Snijders, E.J.B., Wijnants, G.H. and Woft, M.J. (2002), *Study to feasibility of and boundary conditions for floating offshore wind turbines*, Public report 2002-CMC-R43, ECN, MARIN, MSC, Lagerwey the Windmaster, TNO, TUD,.

Caughey, T.K. (1960), "Classical normal modes in damped linear systems", *J. Appl. Mech*., **27**, 269-271.

Chakrabarti, S. (1987), *Hydrodynamics of offshore structures*, Computational mechanics publications.
Chakrabarti, S. (2005), *Handbook of Offshore Engineering*, Elsevier Ocean Engineering Series, 1st Ed.
Chaplin, J.R. http://www.civil.soton.ac.uk/hydraulics/download/downloadtable.htm.
Cook, R.D., Malkus, D.S. and Plesha, M.E. (1989), *Concepts and applications of finite element analysis*, 3rd Ed., John Wiley & Sons, Inc, ISBN 0-471-84788-7.
Haslum, H.A. (1999), *Alternative shape of spar platforms for use in hostile areas*, Offshore Technology Conference.
Henderson, A. and Patel, M. (1998), "Rigid-body motion of a floating offshore wind farm", *Int. J. Ambient Energy*, **19**(3) , 167-180.
IEC 61400-3 (2007), 1st Ed., Wind turbines - Part 3: Design requirements for offshore wind turbines.
Ishihara, T. and Yamaguchi, A. (2005), *Offshore potential in Japan - Offshore resource assessment using a meso-scale model and GIS*, Windtech International, 18-21.
Ishihara, T., Phuc, P.V., Sukegawa, H., Shimada, K. and Ohyama, T. (2007), "A study on the dynamic response of a semi-submersible floating offshore wind turbine system Part 1: water tank test with considering the effect of wind load", *Proceedings of the ICWE12*, Australia.
Jonkman, J.M. (2007), *Dynamic modeling and load analysis of an offshore floating wind turbine*, Department of Aerospace Engineering Sciences, University of Colorado, Ph.D Thesis.
Ju, S.H., Ston,e J.J. and Rowlands, R.E. (1995), "A new symmetric contact element stiffness matrix for frictional contact problems", *Comput. Struct*., **54**(2), 289-301.
Kanda, M., Miyajima, S., Nakagawa, H. and Shimazaki, K. (1998), "A nonlinear coupled response of TLP hull and tendons in waves", *Proceedings of the17th International conference on Offshore Mechanics and Arctic Engineering*, OMAE-0472.
Morison, J.R. *et al*. (1950), "The force exerted by surface waves on piles, Petroleum Transactions", *AIME*, **18**, 149-157.
Motora, S.Z., Koyama, T.O., Fujino, M.T. and Maeda, H.A. (1997), *Dynamics of ships and offshore structures* [in Japanese]
NMRI-National Marine Research Institute: http://www.nmri.go.jp/index_e.html.
Offshore Industry (2009), **2**(4), 48-51.
Offshore Standard DNV-OS-J101 (2004), *Design of offshore wind turbine structures.*
Phuc, P.V. and Ishihara, T. (2007), "A study on the dynamic response of a semi-submersible floating offshore wind turbine system Part 2: Numerical simulation", *Proceedings of the ICWE12*, Australia.
Sarpkaya, T. and Isaacson, M. (1981), *Mechanics of wave forces on offshore structures*, Van Norstrand Reinhold.
Shimada, K., Miyakawa, M., Ohyama, T., Ishihara, T., Fukumoto, Y., Anno, K., Okada, H. and Moriya, Y. (2010), "Preliminal study on optimum design of a Tension Leg platform for the offshore wind generated energy system", *Proceedings of the Renewable Energy Conference*, O-WdOc-2.
Shimizu, M. and Sato, J. (1997), "An analysis of a transmission tower and cable system's sleet-jump", *J. Struct. Eng. - ASCE*, **43,** 403-413**.**
Srinivasan, N., Chakrabarti, S. and Radha, R. (2005), "Damping controlled response of a truss pontoon semisubmersible with heave plates", *Proceedings of the 24th International Conference of OMAE*, Halkidiki, Greece.
Tong, K.C., Quarton, D.C. and Standing, R. (1993), "Float-a floating offshore wind turbine system, in Wind energy conversion", *Proceedings of the 1993 BWEA Wind Energy Conference*, York, England.
Waris, M.B. (2010), *Fully nonlinear finite element model for dynamic response analysis of floating offshore wind turbine system*, Ph. D dissertation, Department of Civil Engineering, The University of Tokyo, Japan.
Wilson, E.L., Penzien, J. (1972), "Evaluation of orthogonal damping matrices", *Int. J. Numer. Meth. Eng*., **4**(1), 5-10.